FOREIGN TECHNOLOGY DIVISION
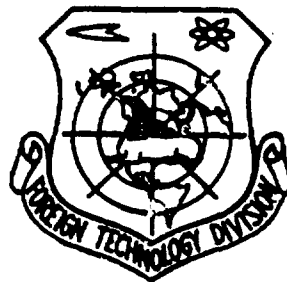
CHARACTERISTICS OF DOUBLE-CANARD AERODYNAMIC
SHAPE CONFIGURATION

by

Wang Bao-xing

DTIC
ELECTE
MAY 1 9 1983
E

83   05   19   020

EDITED TRANSLATION

FTD-ID(RS)T-0659-82   6 April 1983

MICROFICHE NR: FTD-83-C-000503

CHARACTERISTICS OF DOUBLE-CANARD AERODYNAMIC
SHAPE CONFIGURATION

By: Wang Bao-xing

English pages: 13

Source: Lixue yu Shuian, Vol. 2, Nr. 2, 1980,
         pp. 26-30

Country of origin: China
Translated by: SCITRAN
                F33657-81-D-0263
Requester: FTD/TQTA
Approved for public release; distribution unlimited.

GRAPHICS DISCLAIMER

All figures, graphics, tables, equations, etc. merged into this translation were extracted from the best quality copy available.

CHARACTERISTICS OF DOUBLE-CANARD AERODYNAMIC SHAPE CONFIGURATION

Wang Bao-xing
(Tienjin City Optical Instruments Factory)

The double-canard aerodynamic configuration is a new configuration recently developed for air-to-air missiles. The short range dogfight air-to-air missile newly successfully developed by France Matra R550, employs such an aerodynamic configuration.

Starting from the basic mechanism of mutual interference between the foreplane and the canard wing, this paper designed the profile of the canard wing in anticipation of obtaining larger lift effect. Experimental data from wind tunnel tests verified that a relatively large increase in the lift of the canard wing is obtained because of the presence of the foreplane. In addition, more importantly it also revealed a characteristic of this type of aerodynamic configuration-- the pitch moment of the entire missile at small angles of attack shows a favorable nonli..earity. This paper analyzes the advantages of such "nonlinearity" in comparative detail. It is believed that it far exceeds the canard configuration and it is an ideal configuration for dogfight type of air-to-air missiles.

Figure 1 gives the profiles of the dynamometric models used in the tests of the double-canard and canard aerodynamic configurations. It also designated the lift surface in a unified manner.

I. DESIGN OF THE CANARD WING SHAPE AND THE LIFT EFFECT

By comparing the two aerodynamic configurations shown in Figure 1, it is not difficult to see that the double canard aerodynamic configuration is formed by the canard type configuration by installing a foreplane in front of the canard wing. The distance between the foreplane and the canard wing is very short. The mechanism of its mutual interaction is the same as the short spacing, small aspect ratio canard type configuration [1,2] which has been widely studied in recent years.
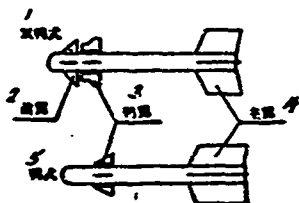
1

Figure 1. Designation of air-
foil nomenclature.
1--double canard type;
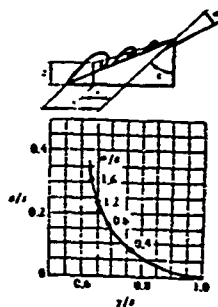2--foreplane; 3--canard wing;
4--main wing; 5--canard type

Figure 2. Correlation between
the front fringe vortex nucleus
position of triangular wing
with attack angle

Previous studies discovered that for a large sweep-back tri-
angular wing, when the attack angle is very small, the flow separates
at the leading edge. Immediately afterward, a high revolution speed
leading edge vortex is established to replace separation disturbance.
When the leading edge sweep-back angle is sufficiently large, the
vortex is very stable. Furthermore, over a wide attack angle range,
the vortex lengthens with increasing attack angle. The nucleus of
the vortex extends towards the inner upper direction of the wing sur-
face. Figure 2 (quoted from [1]) gives the correlations between the
vortex nucleus position and the attack angle α, as well as the
half vortex angle ε of the wing surface. At a far away distance, the
vortex nucleus explodes, which is called a "funnel" in engineering.
Along with increasing attack angle, the "funnel" shifts forward. At
a critical α value, it is shifted to the rear edge of the wing surface.
Experiments proved that when the vortex nucleus is extended into the
pressure rise region, it is easy to form the "funnel". When it extends
into the pressure reducing region, formation of the "funnel" would be
delayed.

In the vortex nucleus, due to the fact that the gas flow revolves
at high speed and the pressure is low, where the vortex nucleus is on
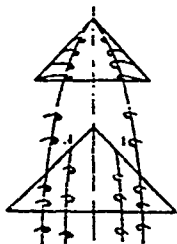
2

Figure 3. Interaction of the front vortices of two wing surfaces which are relatively closely spaced.
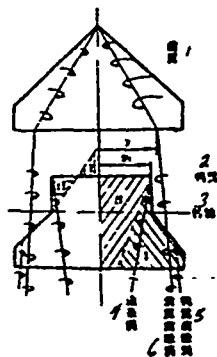

Figure 4. Schematic diagram of vortex series on the foreplane and canard wing
1--foreplane; 2--canard wing; 3--axis of rotation; 4--boundary vortex; 5--foreplane leading edge vortex; 6--canard leading edge vortex

the wing surface, a vortex nucleus suction effect is produced. When the vortex nucleus explodes on the wing surface to form the "funnel", the original neatly arranged flow structure is changed into an irregular distribution if spinning. The pressure increases and subsequently the lift on the wing surface is reduced.

Two closely distanced wing planes (such as the foreplane and canard wing of the double canard type aerodynamic configuration) will mutually produce interference. The interference effect can be separated into two types depending on their relative position: In one, the front fringe vortex dragged from the foreplane surface passes above the rear wing surface; i.e., it passes through the pressure reducing region of the rear wing surface. The vortex nucleus becomes even more stable. In addition, the velocity field induced by the leading edge vortex of the rear wing surface makes the leading edge vortex of the foreplane surface shift downward from the rear portion of the top surface of the rear wing surface. The vortex nucleus becomes even closer to the wing surface. Because the vortex nucleus suction effect produces added lift, under the action of the leading edge vortex of the foreplane, the central portion of the
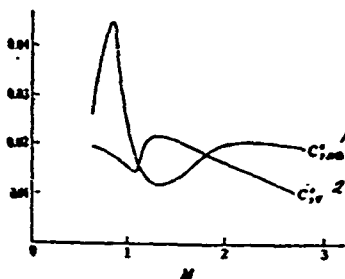
Figure 5. Experimental curve of c_y^{δ} double canard vs. c_y^{δ} canard

rear wing surface induces a very strong down wash while the wing tip part induces very intense up wash. The down wash in the middle is especially intense in the top end portion of the wing surface which will prevent the formation of front edge vortex. However, the up wash part will accelerate the formation of the leading edge vortex. As shown in Figure 3, due to the effect of the leading edge vortex of the foreplane, the leading edge vortex on the rear wing surface is not produced from the vertex but from point A. Moreover, it is even more intense than the one produced when it is isolated.

As for the rear wing surface, the down wash of the middle wing end portion must sacrifice some attack angle which is unfavorable. However, its leading edge vortex is intensified due to the coupling with the leading edge vortex of the foreplane. Furthermore, there are two vortex nuclei passing through its top surface and the vortex suction effect will produce very large added lift. The combined effect is very favorable. In the other version, the foreplane front edge vortex extends to the bottom surface of the rear wing, or extends into the pressure rise region. At this time, the vortex nucleus explosion to form the "funnel" region would be advanced. The "vortex suction effect" of the foreplane leading edge vortex will reduce the lift of the rear wing surface. This coupled effect is unfavorable; it should be avoided.

4

The mutual interaction between the foreplane and the canard wing of the double canard aerodynamic configuration is to realize the first coupling condi' 'escribed above. To require the fore-plane leading edge vortex ·ss through the top surface of the canard wing so that the lift ʋ the canard wing can be improved, it is necessary to carefully design the canard wing shape. Figure 4 is a planar diagram of a foreplane and a canard wing used as the dynamo-metric model of the double canard type aerodynamic configuration. In the following, this special case will be used to explain what considerations are made in the design and the distribution situation of the vortex series.

References [1] and [2] discussed the short spacing canard type configuration of an aircraft. The position of the foreplane is designed to be higher than that of the rear wing so that the first coupling condition can be realized. For a missile, it is not possible to simply use the height of the position. The missile can roll. Look-ing from a certain direction, the foreplane is higher than the canard. By rotating $180°$, it is the reverse. The design shown in Figure 4 is to use the profile of the canard wing and the position of the rotational axis. The canard wing is the control surface which must be deflected. When deflecting by an angle δ the area behind the rotation axis will be lower than the foreplane. If the position of the vortex nucleus of the foreplane leading edge vortex is being dragged from the wing surface $Y > Y_1$ (referring to Figure 4), it is possible to ensure that the foreplane leading edge vortex passes through the top surface of the canard wing. Subsequently, the favorable coupling effect is produced. From Figure 2, we can see that Y, the foreplane half vertex angle ϵ and the attack angle α are correlated. Correspond-ing to α_{max}, if we want to ensure that, within all the attack angle range, the foreplane leading edge vortex can pass through from the top surface of the canard wing, we must make $Y_{min} > Y$.

It has been pointed out before that the effect of foreplane leading edge vortex makes the area of the I part shown in Figure 4 suffer from very intense down wash. The lift created by this part is

5

relatively small. In the design, this portion of the area is elim-
inated and moved to part II. The part in front of the rotation axis
forms a rectangle. The sideline of the rectangular part will produce
a boundary vortex. Thus, there are three vortices on the canard wing
surface: boundary vortex, foreplane leading edge vortex and canard
wing leading edge vortex. They are mutually coupled and reinforce-
ment is obtained. Because of the "vortex nucleus suction effect",
the lift of the canard is made to have a larger increment than that
of the canard wing of the canard type configuration. Table 1 lists
the partial derivatives of the canard wing lift coefficient with res-
pect to the attack angle obtained from the double canard dynamometric
model (without the main wing) wind tunnel tests and the partial deri-
vatives of the canard wing lift coefficient with respect to attack
angle of the canard type configuration (the same missile body, same
canard wing, without main wing). The values are all arranged accord-
ing to $\alpha = \pm2°$ range. The rudder deflection angle is $\delta = 20°$, i.e.,
$\alpha + \delta = 20° \neq 2°$. The data in the table indicates that when the attack
angle is large ($\alpha + \delta$ is the attack angle of the canard wing), the
canard wing boundary vortex, foreplane front edge vortex and the
canard front edge vortex are all intensified. The lift improvement
effect is very significant.

TABLE 1

$\cdot$	0.60	0.70	0.80	0.90	1.00	1.10
$\cdot\,_{in}$	0.0408	0.0265	0.0274	0.0285	0.0313	0.0513
$\cdot\,_{aa}$	0.0462	0.0493	0.0557	0.0479	0.0544	0.0696

Figure 5 gives the partial derivatives of the total missile lift
coefficients obtained from the double canard type and canard type
dynamometric model wind tunnel tests with respect to the rudder
deflection angle δ. C_y^δ is approximately equivalent to the partial
derivative of the canard wing lift coefficient with respect to the
attack angle. In order to facilitate the comparison, the reference
area of C_y^δ is chosen to be the canard wing area (the cantilever seg-
ment). The curve in Figure 5 shows that when $0.6\ M < 1.0$ and $M > 1.8$,

6

$C_{ydouble\ canard}^{\delta} \gg C_{ycanard}^{\delta}$. This further verifies the canard lift improve-
ment effect of the double canard type aerodynamic
configuration shown in Figure 4.

II. THE "NONLINEAR" EFFECT OF THE DOUBLE CANARD TYPE AERODYNAMIC CONFIGURATION

If we say that a foreplane added in front of the canard wing of
the canard type aerodynamic configuration to improve the canard wing
lift is the expected result of the double canard type aerodynamic
configuration, then the results of wind tunnel tests revealed another
important unexpected characteristic--the pitch moment M_z shows a
favorable nonlinearity at small attack angles. Figure 6 shows the
typical $M_z - \alpha$ wind tunnel test curve of the double canard type aero-
dynamic profile dynomometric model. On the curve at small attack
angles (AA' and LL' segments), M_z increases with increasing attack
angle ($M_z^{\alpha} > 0$). Only when going beyond point A' (or point L'), M_z
then decreases with increasing attack angle α ($M_z^{\alpha} < 0$). This "non-
linearity" has the following advantages (referring to Figure 6).

(1) under the same static stability, it is possible to obtain a
larger equilibrium attack angle as compared to the canard type aero-
dynamic configuration so that a larger transverse overload can be
attained. Point A is the pitch moment generated by the 18° deflection
of the canard wing ($\alpha = 0°$). The equilibrium point ($M_z = 0$) of the
double canard type aerodynamic configuration is B,
$\alpha_{double\ canard\ equilibrium} = 16°$. For the canard type configuration, the
initial M_z ($\delta = 18°$, $\alpha = 0°$) and the M_z^{α} near the equilibrium point are
the same as those of the double canard type configuration because its
$M_z-\alpha$ curve is linear. The equilibrium point is B'. From Figure 5,
we obtain $\alpha_{equilibrium\ canard} = 12°$. Therefore,
$\Delta\alpha = \alpha_{equilibrium.double\ canard} - \alpha_{equilibrium.canard} = 4°$

This also means that when $M = 0.9$ and the canard wing deflects
by 18°, the same pitch moment is created. Under the same static
stability condition (identical M_z^{α}), due to the nonlinearity of the
$M_z - \alpha$ curve of the double canard type also dynamic configuration,

7

an additional 4° of equilibrium attack angle is produced as com-
pared to the canard type configuration, which corresponds to an
increase in transverse overload by 1/4.

If the areas of the canard wings are identical, considering
that the canard wing of the double canard type aerodynamic configur-
ation is high (from Figure 5 we find that when $M = 0.9$, $C_{y \, doublecanard}^{\delta}$
$= 2 \, C_{y \, canard}^{\delta}$) for the same deflection of 18°, then
$M_{Z \, canard} \, (\alpha = 0, \, \delta = 18°) = \frac{1}{2} \, M_{Z \, double \, canard} \, (\alpha = 0, \, \delta = 18°)$

The starting point of the canard type configuration is at C.
If the same M_Z^{α} is to be maintained at the equilibrium point, then
the equilibrium point is at D, $\alpha_{equilibrium.canard} = 6°$.

$\Delta\alpha = \alpha_{equilibrium.double \, canard} - \alpha_{equilibrium.canard} = 10°$

Figure 6. The pitch moment
curve of the double canard
type aerodynamic configura-
tion
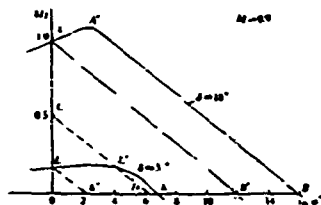
The maximum useable overload is
$$n_{max} = (C_y^{\alpha} \cdot \alpha_{equilibrium} + C_y^{\delta} \, \delta_{max}) \, \frac{q \cdot s}{w}$$

where C_y^{α} - partial derivative of the lift coefficient of the missile
with respect to the attack angle α;

C_y^{δ} - partial derivative of the lift coefficient of the missile
with respect to the rudder deflection angle δ;

δ_{max} - maximum rudder deflection angle;

$\alpha_{equilibrium}$ - equilibrium attack angle at maximum rudder
deflection angle;

q - dynamic pressure; s - reference area, w - missile weight

By taking into account that $C_y^{\alpha} \cdot \alpha_{equilibrium} \gg C_y^{\delta} \cdot \delta_{max}$, we
can consider in approximation that the maximum useable overload is
proportional to the maximal equilibrium attack angle. This also

8

means that when the canard wing area is identical anᵤ the deflection
is the same 18°, under the condition that the same static stability
is to be maintained, the equilibrium attack angle of the double
canard type aerodynamic configuration is larger by 10° than the equi-
librium attack angle of the canard type aerodynamic configuration.
The transverse useable overload increases approximately 1.6 times.

(II) The dynamic response speed is improved as compared to the
canard type configuration. When the canard wing is deflected by 3°,
a pitch moment M_z is produced ($\alpha = 0$, $\delta = 3°$) which is the point L in
Figure 6. As the attack angle starts to increase, finally it reaches
the static equilibrium point K. The double canard type aerodynamic
configuration varies from the solid line LL' to point K. In the
segment LL', with increasing α, M_z also increases. Consequently, the
rate of the attack angle increase is also increased. Beyond point L',
with increasing attack angle, M_z decreases. The value of M_z^α at point
K is negative; therefore, K is a static stability point. If it is
the canard type configuration, the M_z^α at the equilibrium point is
identical; then it varies from point L to point K' along a straight
line. Thus, as α increases, M_z would decrease linearly and the rate
of attack angle increase would also decrease. From these results, we
can see that the dynamic response speed of the double canard type
aerodynamic configuration is much faster than that of the canard type
aerodynamic configuration.

This nonlinearity is produced due to the addition of the fore-
plane. Figure 7 lists the forces exerted on various parts of the
double canard type missile. From the diagram we obtain

$$M_z = Y_{head} X_1 \sin \alpha + Y_{foreplane} X_2 \sin \alpha + Y_{canard} X_3 \sin (\alpha-\epsilon_1) - Y_{main\ wing} X_4 \sin (\alpha - \epsilon_2)$$

where Y_{head} – lift of the head; $Y_{foreplane}$ – lift of the foreplane;
Y_{canard} – lift of the canard wing; X_1 – distance between Y_{head} and
the center of gravity; X_2 – distance between $Y_{foreplane}$ and the cen-
ter of gravity; X_3 – distance between Y_{canard} and the center of gra-
vity; X_4 – distance between $Y_{main\ wing}$ and the center of gravity; ϵ_1 –
the average down-wash angle at the canard wing; ϵ_2 – the average
down wash angle at the main wing.

When α is relatively small, $\sin \alpha = \alpha$. The above equation can be rewritten as

$$M_z = [C_y^a \text{ head } S_{head} \, X_1 \, \alpha^2 + C_y^\alpha \text{ foreplane } \cdot \delta_{foreplane} \, X_2 \, \alpha^2$$
$$+ C_y^\alpha \text{ canard } S_{canard} \, X_3 \, (\alpha = \epsilon_1)(\alpha + \delta - \epsilon_1) - C_y^\alpha \text{ main wing } S_{main \, wing}$$
$$X_4 \, (\alpha - \epsilon_2)] \, q$$

Under the condition that δ = const and $(S_{foreplane} + S_{canard})$ is not much smaller than $S_{main \, wing}$ (such as in the double canard type aerodynamic configuration dynamometric model $S_{foreplane} + S_{canard}$ = 0.8 $S_{main \, wing}$ shown in Figure 1), $(\alpha + \delta/2 = \epsilon_1) \gg (\alpha - \epsilon_2)$ in the vicinity of small α, then $M_z^\alpha > 0$. When α is relatively large, $(\alpha + \delta/2 - \epsilon_1)$ and $(\alpha - \epsilon_2)$ are not too different in magnitude, $S_{main \, wing}$ X_4 is relatively large. Therefore, the last term in the above formula has the major effect. Hence, $M_z^\alpha < 0$. which is the cause of nonlinearity. In the canard type aerodynamic configuration, due to the fact that the canard wing area is small, the main wing lift always has the major effect. Therefore, M_z^α is always less than zero.

Figure 7. Schematic diagram
of forces exerted on various
parts of a double canard
type missile
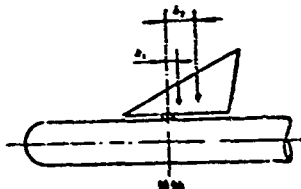1--Y head; 2--Y foreplane;
3--Y canard; 4--Y main wing

Figure 8. Hinge moment of the
canard type control
1--rotation axis

III. CONTROL CHARACTERISTICS OF THE DOUBLE CANARD TYPE AERODYNAMIC CONFIGURATION

It has been pointed out previously that with regard to the canard wing of a double canard type configuration, if the shape and the rotation axis position are designed properly, the efficiency of the

10

canard wing (C_y^δ) can be improved. Another requirement as a control
surface is that hopefully the hinge moment is small. Thus, it is
possible to have a service mechanism which is not too large and
heavy in order to satisfy the required characteristics in the mean-
time. It is commonly known that the key to reducing the hinge
moment is to reduce the variation of the pressure center of the
canard wing under various conditions. For example, as in canard
type control, the canard wing is triangular (as shown in Figure 8)
and the pressure center in a subsonic flow is located at between 0.3-
0.4 average aerodynamic chord. In supersonic flows, it is close to
0.5 average aerodynamic chord. The control stability requires that
the rotation axis of the canard wing ought to be located in front of
the pressure center. The maximum hinge moment is (see Figure 8).

$$M_{hinge} = - ph_2 = - ph_1 - P(h_2 - h_1)$$

where: M_{hinge} - maximum hinge moment; P - maximum perpendicular
force component on the surface of the canard wing; h_1 - minimum dis-
tance between the subsonic pressure center and the rotation axis;
h_2 - maximum distance between the supersonic pressure center and the
rotation axis.

If the maximum pressure center displacement $h_2 - h_1$ is very small,
as long as h_1 is designed to be sufficiently small, it is possible
to reduce the hinge moment. The pressure center displacement of
canard type control is about 0.2 average aerodynamic chord length.
Therefore, it is difficult to make the hinge moment very small.

The variation of the pressure center position of the double
canard type aerodynamic configuration with velocity is not too large.
Qualitatively, we can explain in this way that in zone A of the
canard wing (referring to Figure 4) the top surface is under the
influence of the foreplane front edge vortex, canard wind boundary
vortex and canard wing front edge vortex. The suction effect of the
vortex nucleus makes the lift increase in this region. In addition,
it is located in the upwash region of the incoming flow, and the
attack angle also increases. Therefore, zone A has a large contribu-
tion to the lift of the entire canard wing. Zone B does not have

11

vortex suction and is situated in the downwash zone of incoming flow. It has very small contribution to the canard wing lift. The combined effect of zones A and B makes the subsonic pressure center to approach 0.5 average aerodynamic chord length. For supersonic flow, it is even closer to 0.5 average aerodynamic chord length. This indicates that the variation of pressure center of the canard wing in the double canard type aerodynamic configuration with the Mach number is very small. Its pressure center position is very difficult to obtain accurately by calculation. It must be determined with the assistance of wind tunnel tests. With regard to the canard wing profile shown in Figure 4, if it is designed properly, the variation of the pressure center position X is

$$0.45 b_{AK} < X < 0.5 b_{AK} \qquad\qquad 30$$

where X is the distance from the starting point of the average aerodynamic chord to the pressure center, and b_{AK} is the average aerodynamic chord length of the cantilever segment. The maximum variation of the pressure center with velocity is $h_2 - h_1 = 0.05 b_{AK}$, which is 1/4 of that of the canard type aerodynamic configuration. If the rotation axis is designed to be in the $0.43 b_{AK}$ position, then

$$M_{hinge \cdot double \ canard} = 0.07 \ pb_{AK}$$
$$M_{hinge \cdot canard} = 0.22 \ pb_{AK}$$

Under the condition of identical aerodynamic force P, the hinge moment of the double canard type configuration is only 1/3 that of the canard type configuration.

Summarizing the above description, the double canard type configuration can attain higher maneuverability and faster dynamic response speed than the canard type configuration, while the required rudder power is less. Therefore, it is an ideal configuration for a dogfight type air-to-air missile. The low altitude ground-to-air missile with high maneuverability requirements can also adopt this configuration.

12

REFERENCES

[1] Hermann Behrbohm. Foreign Aeronautical Technology, No. 44
     (1975), 12-43

[2] Roed, A., Foreign Aeronautical Technology, No. 44 (1975),
     44-47